International Journal of Legal Medicine (2022) 136:1483–1494
https://doi.org/10.1007/s00414-022-02840-y

ORIGINAL ARTICLE

DXAGE 2.0 — adult age at death estimation using bone loss in the proximal femur and the second metacarpal

Francisco Curate[1,2,3] · David Navega[2,4] · Eugénia Cunha[2,4] · João d'Oliveira Coelho[2,5]

Received: 20 April 2022 / Accepted: 16 May 2022 / Published online: 27 May 2022

Abstract

The accurate age at death assessment of unidentified adult skeletal individuals is a critical research task in forensic anthropology, being a key feature for the determination of biological profiles of individual skeletal remains. We have previously shown that the age-related decrease of bone mineral density (BMD) in the proximal femur could be used to assess age at death in women (Navega et al., J Forensic Sci 63:497–503, 2018). The present study aims to generate models for age estimation in both sexes through bone densitometry of the femur and radiogrammetry of the second metacarpal. The training sample comprised 224 adults (120 females, 104 males) from the "Coimbra Identified Skeletal Collection," and different models were generated through least squares regression and general regression neural networks (GRNN). The models were operationalized in a user-friendly online interface at https://osteomics.com/DXAGE2/. The mean absolute difference between the known and estimated age at death ranges from 9.39 to 13.18 years among women and from 10.33 to 15.76 among men with the least squares regression models. For the GRNN models, the mean absolute difference between documented and projected age ranges from 8.44 to 12.58 years in women and from 10.56 to 16.18 years in men. DXAGE 2.0 enables age estimation in incomplete and/or fragmentary skeletal remains, using alternative skeletal regions, with reliable results.

Keywords Dual X-ray absorptiometry · Radiogrammetry · Biological profile · Forensic anthropology · Bioarcheology

Introduction

The accurate age at death estimate of unknown skeletons of adult individuals is a crucial research task in both bioarcheology and forensic anthropology, being a key feature for the determination of population demographic structures and biological profiles of individual remains [2, 3]. Current adult aging routines are traditionally based on macroscopic observations of the degenerative ("wear and tear") changes in four skeletal regions: the pubic symphysis [4–8], the auricular surface [9–12], cranial sutures [13, 14], and sternal rib ends [15–17]. However, a plethora of other skeletal regions and methods are also used — in combination with long-standing reference methods, or independently — to estimate age at death in adults. These encompass, among others, molecular clocks in ancient proteins [18], the degeneration of the acetabulum [19, 20], amino acid racemization in dental tissues [21, 22], tooth-root translucency [23], dental attrition [24, 25], the ratio of the pulp/tooth area in canines [26], and bone histology [27, 28].

Unfortunately, most skeletal indicators are unreliable, showing weak and irregular associations with age, echoing the complexity of the aging process [29, 30]. Individual and population differences during biological senescence stem from a reticulate of factors and interactions at the genetic, sociocultural, and environmental levels [29, 31, 32]. Moreover, existing age estimation techniques often present methodological problems, such as the subjective nature of user-observation and subsequent lower reproducibility [4, 33] and the application of inappropriate sampling and statistical procedures [3, 34, 35].

✉ Francisco Curate
fcurate@uc.pt; franciscocurate@gmail.com

1 Research Centre for Anthropology and Health, Department of Life Sciences, University of Coimbra, Coimbra, Portugal

2 Laboratory of Forensic Anthropology, Centre for Functional Ecology, Department of Life Sciences, University of Coimbra, Coimbra, Portugal

3 School of Technology, Polytechnic Institute of Tomar, Tomar Macao, Portugal

4 National Institute of Legal Medicine and Forensic Sciences, I.P. (INMLCF, I.P.), South Branch, Lisbon, Portugal

5 Institute of Cognitive and Evolutionary Anthropology, University of Oxford, Oxford, UK

Scientific organizations and individual researchers alike have been advocating for more objective, less observer-dependent, age estimation methods, with a concomitant exploration of innovative statistical approaches [3, 33, 36–38]. New methodologies for age estimation in skeletal remains are thus needed to address these concerns.

Bone mass decrease with age is a universal phenomenon — in individuals of both sexes from different populations, e.g., [39–43]. Age affects bone loss through direct and indirect mechanisms, including remodeling imbalance, secondary hyperparathyroidism, decline in the intestinal production of the active metabolite of vitamin D, and reduction in bone tissue repair [44–46]. Age-specific bone remodeling occurs in different skeletal regions and types of bone tissue — i.e., trabecular and cortical — at dissimilar rates, and macroscopically observable features of bone loss have long been used to develop aging standards in adults, e.g., [47–54]. Recently, bone densitometry has been used to develop and test methods for age at death estimation based on the association between bone mineral density (BMD) and age [55–58].

We have previously shown that the age-associated decrease of bone mineral density (BMD) at the proximal extremity of the femur could be considered to estimate age at death in women of Portuguese descent [1]. Published results emphasized the potential of dual-energy X-ray absorptiometry (DXA), data modeling through artificial neural networks (ANN), and a user-friendly online interface named DXAGE (http://osteomics.com/DXAGE/), to attain accurate and reproducible estimates of age at death in skeletal remains of adults. Nevertheless, DXAGE was only designed for age estimation of adult women. As such, the present study aims to provide models for age estimation of both sexes through bone densitometry at the proximal femur. Also, age-related cortical bone loss at the second metacarpal is well established in both modern and archeological samples [59–65] — but, except for Kimura's (1992) method, cortical bone loss with age at the second metacarpal has not been used for age estimation in skeletal remains of adults. Accordingly, another objective of this study is to assess the potential of bone loss at the second metacarpal to estimate age at death in adult individuals. The development of an online application (DXAGE 2.0) featuring different statistical models for age estimation using BMD at the proximal femur and second metacarpal cortical index (MCI) constituted an ancillary objective.

Materials and methods

Sample

The training study base comprised 224 adults (120 females and 104 males) from the "Coimbra Identified Skeletal Collection" (CISC; Cunha and Wasterlain, [66]). Documented ages at death ranged from 20 to 96 years old (Table 1). Sampled individuals were Portuguese nationals and for the most part were non-specialized manual workers with low socioeconomic status. They were buried for at least 5 years — as a rule, after that period, the bodies were exhumed — in earth-cut shallow graves at the Conchada Municipal Cemetery (Coimbra, Portugal).

Data collection

The left femur and left second metacarpal of each individual were evaluated through dual X-ray absorptiometry and conventional radiogrammetry, respectively. Individuals without gross post-depositional modifications and/or obvious disease modifications at the skeletal sites of interest were the only ones included in the sample.

Osteodensitometry (also identified as bone densitometry) was attained with a Hologic QDR 4500C Elite densitometer (available issued formulae should be used to convert BMD values measured on a densitometer from other manufacturers, e.g., GE Healthcare or Nordland). Femora were placed anteroposteriorly, aligning the diaphysis to the densitometer's central axis, on a low-density cardboard box, on top of 10 cm of rice (see [1, 68]). Regarding osteodensitometry, the proximal extremity of the femur is usually separated into distinctive regions of interest (ROI): total hip, trochanteric and intertrochanteric/proximal diaphysis regions, femoral neck, and Ward's area. The total hip area of the femur (also identified in the medical literature as the total proximal femur region) stems from the aggregate of three specific parts: trochanteric region, intertrochanteric/proximal diaphysis regions, and neck (Fig. 1) [67]. In this study, bone area (cm^2), bone mineral content (BMC, g), and bone mineral density (BMD, g/cm^2) were determined through a semi-automatic procedure in three of the ROI: femoral neck, Ward's area, and total hip. BMD at these sites was used to construct the models for the prediction of age at death.

Table 1 Age and sex distribution of the study sample of the Coimbra Identified Skeletal Collection (CISC)

Age class	Females		Males	
	N	%	*N*	%
20–29	15	12.5	14	13.5
30–39	18	15.0	15	14.4
40–49	21	17.5	15	14.4
50–59	19	15.8	14	13.5
60–69	14	11.7	18	17.3
70–79	18	15.0	21	20.2
80 +	15	12.5	7	6.7

Sample size, *N*; percentage, %

Fig. 1 Densitometry report featuring, among others, bone mineral density values, T-scores and Z-scores at the femoral neck, Ward's area, and total hip

DXA Results Summary:

Region	Area (cm^2)	BMC (g)	BMD (g/cm^2)	T - Score	PR (%)	Z - Score	AM (%)
Neck	5.81	3.81	0.656	-2.0	71	-1.2	81
Troch	13.07	8.34	0.638	-1.1	82	-0.8	86
Inter	24.67	20.84	0.845	-1.9	71	-1.7	74
Total	**43.55**	**33.00**	**0.758**	**-1.8**	**73**	**-1.4**	**78**
Ward's	1.30	0.67	0.512	-1.9	65	-0.5	89

Total BMD CV 1.0%
WHO Classification: Osteopenia
Fracture Risk: Increased

Conventional radiogrammetry was employed to determine the cortical index (MCI) at the mid-diaphysis of the second metacarpal, according to [69]:

$$MCI = \frac{\text{Diaphysis total width} - \text{Medullary width}}{\text{Diaphysis tota lwidth}}$$

Radiographs were acquired in a Senographe DS digital radiographic device (GE Healthcare; focal length 50 cm, Kv 27–30 and mAseg 14–20, according to the features of each individual metacarpal), and all measurements were accomplished through the Centricity DICOM Viewer 3.1.1 software.

The data that sustain the results of this study are attainable from the corresponding author upon reasonable request.

Statistical analysis

Descriptive statistics, namely group means, standard deviation, and 95% confidence intervals for the mean, were assessed. Conventional least squares regression analysis [70] and an adapted General Regression Neural Network [71] were employed to assign the different variables (i.e., BMD Total, BMD Neck, BMD Ward, and MCI) toward a model of age at death estimation.

The plainest arrangement of regression (i.e., single linear regression) presupposes a linear association between two variables that can be denoted by the ensuing equation:

$$Y = \alpha + \beta X + \epsilon$$

in which X indicates the independent variable, Y the dependent variable, α the value of Y when X corresponds to zero, β the slope in Y with X, and ϵ features the non-systematic error in Y [38, 72]. The model assumes that Y shows statistical uncertainty, and errors present a normal distribution around the real values with constant variance, whereas X is error-exempted or virtually error-exempted [73]. Predictive variables selection was performed with a stepwise approach, and collinear attributes, if any, were removed from the final models.

A general regression neural network (GRNN) was also used to model BMD and MCI variables as predictors of age at death. This ANN aims to simulate the associative memory, comprising distinct layers: input, pattern, summation, and output [71, 74]. The input layer matches the BMD and MCI vectors to predict age, while in the pattern layer, the input is equated with additional instances stored at the network's memory. Each instance, or pattern, present in the network is operated in the same way as an artificial neuron initiated by a radial basis function. The layers summation and output provide a regression surface and an assessment of age at death employing the pondered average of memory stockpiled examples. The activation values of the radial basis function linked to the artificial neurons support the factors of ponderation. Considering a matrix of predictors X and an outcome variable Y, the estimate of the network $Y(X)'$ can be depicted as follows:

$$Y(X) = \frac{\sum_{i=1}^{n} Y^i e^{-\frac{D_i^2}{2\sigma^2}}}{\sum_{i=1}^{n} e^{-\frac{D_i^2}{2\sigma^2}}}$$

in which D_i^2 is the distance between the vector of the input layer and the ith example pre-deposited in the pattern layer's memory, and σ^2 is a smoothing parameter controlling the projected density and regulating the information volume surrounding the artificial neurons.

The preparation of these models was implemented with Brent's algorithm, in combination with an arrangement of cross-validation ($K = n - 1$) and used the entire sample. The probabilistic estimation of age at death is considered the most appropriate [75, 76]; thus, the ANN employed

was adapted to produce, not only the conditional mean, but also an estimate of the a posteriori distribution. By adopting a probabilistic framework, the estimation of age at death can be mathematically expressed as follows:

$$f(y|x) = \frac{f(x|y)f(y)}{f(x)} = \frac{f(x|y)f(y)}{\int_a^b f(x|y)f(y)dy}$$

The third and fourth layers of the artificial neural network have to be altered to obtain $f(y|x)$ and to allow for the assessment of $f(x|y)$ through a kernel function of Gaussian type. The concluding age at death prediction is attained by the quantile estimation related to the a posteriori distribution.

Results

BMD shows a graded decrease with increasing age at all sites. Results by sex and age class are summarized in Table 2, Table 3 Table 4. In women, BMD Total exhibits a negative and moderate linear association with age at death (Pearson's $r = -0.696$; $p < 0.001$), whereas both BMD at the neck of the femur (Pearson's $r = -0.743$; $p < 0.001$) and BMD at the Ward's area (Pearson's $r = -0.765$; $p < 0.001$) present a negative and strong correlation with age (Fig. 2). Relative change between the first age class (20–29 years) and the oldest age group (80 + years) oscillates between 39.0% (BMD Total) and 56.9% (BMD Ward). Among men, BMD Total (Pearson's $r = -0.543$; $p < 0.001$) and BMD Neck (Pearson's $r = -0.660$; $p < 0.001$) decline moderately with age, while BMD Ward shows a strong and negative linear correlation with age (Pearson's $r = -0.718$; $p < 0.001$;

Table 2 Mean values of bone mineral density at the total hip (BMD_{Total}) according to sex and age class (CISC)

Age class	Females				Males			
	Mean	SD	95% CI	N	Mean	SD	95% CI	N
20–29	0.916	0.11	0.855–0.977	15	1.045	0.09	0.991–1.097	14
30–39	0.931	0.10	0.882–0.981	18	0.948	0.14	0.869–1.027	15
40–49	0.843	0.12	0.786–0.899	21	0.895	0.17	0.802–0.988	15
50–59	0.781	0.12	0.721–0.840	19	0.872	0.13	0.796–0.947	14
60–69	0.746	0.12	0.675–0.817	14	0.840	0.11	0.784–0.894	18
70–79	0.708	0.09	0.662–0.755	18	0.764	0.13	0.703–0.824	21
80 +	0.559	0.16	0.504–0.614	15	0.804	0.16	0.654–0.955	7

Table 3 Mean values of bone mineral density at the femoral neck (BMD_{Neck}) according to sex and age class (CISC)

Age class	Females				Males			
	Mean	*SD*	95% CI	*N*	Mean	*SD*	95% CI	*N*
20–29	0.813	0.12	0.746–0.880	15	0.953	0.07	0.912–0.996	14
30–39	0.842	0.10	0.790–0.893	18	0.851	0.12	0.785–0.918	15
40–49	0.734	0.12	0.680–0.788	21	0.757	0.15	0.673–0.841	15
50–59	0.674	0.09	0.629–0.720	19	0.720	0.11	0.659–0.780	14
60–69	0.611	0.11	0.549–0.672	14	0.707	0.11	0.651–0.763	18
70–79	0.596	0.08	0.558–0.634	18	0.630	0.10	0.590–0.671	21
80 +	0.474	0.07	0.433–0.515	15	0.661	0.13	0.544–0.781	7

Table 4 Mean values of bone mineral density at Ward's area (BMD_{Ward}) according to sex and age class (CISC)

Age class	Females				Males			
	Mean	*SD*	95% CI	*N*	Mean	*SD*	95% CI	*N*
20–29	0.744	0.21	0.627–0.861	15	0.794	0.10	0.734–0.853	14
30–39	0.738	0.13	0.674–0.802	18	0.691	0.15	0.606–0.776	15
40–49	0.609	0.12	0.555–0.664	21	0.584	0.14	0.506–0.662	15
50–59	0.491	0.12	0.433–0.550	19	0.524	0.09	0.471–0.578	14
60–69	0.429	0.13	0.355–0.503	14	0.499	0.09	0.456–0.542	18
70–79	0.398	0.06	0.367–0.429	18	0.430	0.08	0.391–0.468	21
80 +	0.321	0.08	0.280–0.363	15	0.445	0.05	0.324–0.566	7

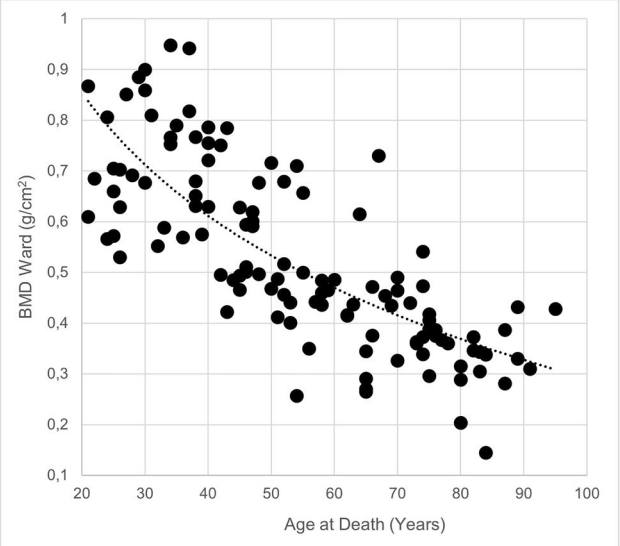

Fig. 2 Strong negative association between bone mineral density at Ward's area (g/cm.^{3}) and age at death in females (CISC)

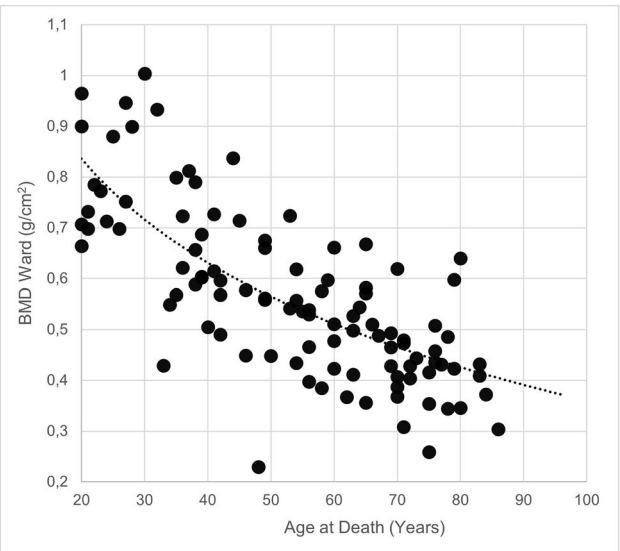

Fig. 3 Strong negative association between bone mineral density at Ward's area (g/cm.^{3}) and age at death in males (CISC)

Fig. 3). BMD variation between the youngest and oldest age classes is lesser than in women, fluctuating between 23.1% (BMD Total) and 44.0% (BMD Ward). MCI also decreases with increasing age at death in both sexes (Table 5), with a negative and moderate linear association in the women's group (Pearson's $r = -0.582$; $p < 0.001$), and a weak, negative, correlation among men (Pearson's $r = -0.202$; $p = 0.040$). Relative variation between the youngest and oldest age classes is 39.9% in women and 21.0% in men.

A conventional least squares regression analysis was conducted, and three age estimation models — tailored for each sex and also for individuals whose biological sex is not known — were generated (Table 6). Goodness-of-fit statistics for the different linear regression models used to predict adult age at death are summarized in Table 7. The mean absolute difference between the known and predicted age at death ranges from 9.39 to 13.18 years among women and 10.33 to 15.76 among men. The best linear regression models combine BMD Ward with MCI, while those that employ only the metacarpal cortical index present the poorer performance.

A modified general regression neural network was employed to generate different models for age estimation. A total of 15 models for each sex — and for individuals with unknown sex — were created. Measures of prediction accuracy for the age at death predicting method are summarized in Table 8. In women, the mean absolute difference between documented and projected age ranges from 8.44 to 12.58 years, while in men, the difference ranges from 10.56 and 16.18 years, contingent to the variables employed to generate the models. As a rule, models relying on BMD variables show increased accuracy: a model with BMD at the neck and BMD Ward exhibits the best performance in women, and the model that uses only BMD measured at Ward's is superlative in men. The least efficient models include those that only use the metacarpal cortical index, followed by those that employ BMD Total in isolation.

All models were contrived as a new online application — DXAGE 2.0, freely available at http://osteomics.com/DXAGE2/ — that enables a user-friendly and interactive routine for age estimation with BMD and MCI values. In

Table 5 Mean values of metacarpal cortical index (MCI) according to sex and age class (CISC)

Age class	Females				Males			
	Mean	*SD*	95% CI	*N*	Mean	*SD*	95% CI	*N*
20–29	53.99	10.01	48.44–59.54	15	55.66	12.90	48.22–63.11	14
30–39	52.56	9.19	47.98–57.13	18	59.95	12.14	53.23–66.68	15
40–49	56.54	11.60	51.26–61.82	21	55.30	11.15	49.12–61.47	15
50–59	50.48	7.77	46.74–54.23	19	60.09	13.95	52.03–68.14	14
60–69	41.77	9.77	36.13–47.42	14	53.53	13.95	52.04–68.14	18
70–79	43.01	6.45	39.80–46.22	18	52.67	11.18	47.58–57.75	21
80+	32.45	7.11	28.51–36.38	15	43.95	6.55	37.89–50.00	7

Table 6 Age estimation models with least squares regression

Model	Regression equation	*SEE*	*R*	*N*
F1	AGE = 109.70 − (63.69 × BMDWard) − (0.45 × *MCI*)	11.79	0.800	120
F2	AGE = 95.32 − (77.11 × BMDWard)	12.66	0.765	120
F3	AGE = 100.44 − (0.97 × *MCI*)	15.99	0.582	120
M1	AGE = 109.54 − (81.38 × BMDWard) − (0.18 × *MCI*)	13.07	0.727	104
M2	AGE = 100.81 − (83.03 × BMDWard)	13.24	0.718	104
M3	AGE = 71.19 − (0.31 × *MCI*)	18.64	0.202	104
U1	AGE = 106.38 − (73.42 × BMDWard) − (0.24 × *MCI*)	12.66	0.756	224
U2	AGE = 97.32 − (78.93 × BMDWard)	12.96	0.742	224
U3	AGE = 84.53 − (0.60 × *MCI*)	17.99	0.387	224

F females, *M* males, *U* unknown sex, *BMD Ward* bone mineral density at Ward's area, *MCI* metacarpal cortical index, *SEE* standard error of the estimate, *R* Pearson correlation coefficient, *N* sample size

Table 7 Statistical metrics for different linear regression models used to estimate age at death through bone mineral density (BMD Ward) and metacarpal cortical index (MCI)

Model	Females						Males					
	MAE	*RMAE*	*MAPE*	*RMSE*	*RRMSE*	*ARSQ*	*MAE*	*RMAE*	*MAPE*	*RMSE*	*RRMSE*	*ARSQ*
Ward	10.06	0.60	23.47	12.61	0.64	0.58	10.38	0.64	23.65	13.18	0.70	0.51
MCI	13.18	0.78	31.64	15.93	0.81	0.33	15.76	0.97	39.13	18.54	0.98	0.03
Ward, MCI	9.39	0.56	21.99	11.74	0.60	0.63	10.33	0.64	23.78	13.00	0.69	0.52

MAE mean absolute error, *RMAE* relative mean absolute error, *MAPE* mean absolute percent error, *RMSE* root of mean square error, *RRMSE* relative root of mean square error, *ARSQ* pseudo-coefficient of determination (adjusted R^2)

Table 8 Statistical metrics for different artificial neural network models used to estimate age at death through bone mineral density (BMD Total, Neck, and Ward) and metacarpal cortical index (MCI)

Model	Females						Males					
	MAE	RMAE	MAPE	RMSE	RRMSE	ARSQ	MAE	RMAE	MAPE	RMSE	RRMSE	ARSQ
Total	11.20	0.67	25.23	14.25	0.72	0.47	13.54	0.84	31.79	16.42	0.86	0.25
Neck	10.02	0.60	22.69	12.70	0.65	0.58	11.42	0.70	26.14	14.59	0.77	0.41
Ward	8.88	0.53	19.56	11.38	0.58	0.66	10.56	0.65	23.92	13.33	0.70	0.50
MCI	12.58	0.75	29.63	15.46	0.79	0.38	16.18	1.00	40.14	19.09	1.00	0.02
Total, Neck	10.48	0.62	23.93	13.25	0.67	0.54	12.06	0.74	27.77	14.93	0.78	0.37
Total, Ward	8.79	0.52	19.31	11.31	0.57	0.66	10.90	0.67	24.13	14.24	0.75	0.43
Total, MCI	9.95	0.59	23.25	12.67	0.64	0.58	13.79	0.85	32.36	16.75	0.88	0.21
Total, Neck, Ward	8.63	0.51	19.26	11.11	0.56	0.67	10.97	0.68	24.55	13.85	0.73	0.45
Total, Neck, MCI	9.61	0.57	22.60	12.29	0.62	0.60	12.39	0.76	29.13	15.13	0.80	0.35
Total, Ward, MCI	8.65	0.51	20.05	11.17	0.57	0.67	11.29	0.70	26.49	14.05	0.74	0.44
Neck, Ward	8.44	0.50	18.25	10.61	0.54	0.70	10.78	0.66	24.28	13.62	0.72	0.48
Neck, MCI	9.61	0.57	22.53	12.35	0.63	0.60	11.91	0.73	27.72	14.88	0.78	0.38
Neck, Ward, MCI	8.62	0.51	19.95	11.15	0.57	0.67	11.00	0.68	25.55	13.86	0.73	0.45
Ward, MCI	8.70	0.52	20.11	11.19	0.57	0.67	10.87	0.67	25.38	13.65	0.72	0.48
All variables	8.57	0.51	19.91	11.26	0.57	0.66	11.24	0.69	26.07	13.99	0.73	0.44

MAE mean absolute error, *RMAE* relative mean absolute error, *MAPE* mean absolute percent error, *RMSE* root of mean square error, *RRMSE* relative root of mean square error, *ARSQ* pseudo-coefficient of determination (adjusted R^2)

the case of GRNN models, DXAGE 2.0 displays the most probable point estimate for age at death, as well as a credible interval featuring the lowest and highest values of age predicted (Fig. 4). The application facilitates the exclusion of any of the variables when appropriate. The least squares regression module (GLM) features a map of data points that supports measurement validation.

Discussion

This study elaborates a previous method [1] by extending its application to adult males, introducing metacarpal cortical bone loss features to the age estimation models, and adding least squares regression analysis to the statistical models. Bone mineral density declines with age, a general pattern identified in epidemiological and anthropological samples, e.g., [39, 40, 42, 43, 68, 77–80]. Age-related cortical bone decline at the second metacarpal has been also observed in both contemporary and historical assemblages, e.g., [59, 61–63, 81]. Bone loss continues even during old age [41, 82], a feature that is useful for the assessment of age in older individuals.

Bone decline with age seems more evident in women and in the proximal femur — and that explains the better results found in the models designed for females and in those using BMD features instead of MCI. Before puberty, there are no consistent differences in bone mass between women and men [83, 84] with sex heterogeneity in bone morphology and mass resulting from the later onset and prolonged extent of puberty in males [85]. After the attainment of peak bone mass, age-related bone loss occurs in both sexes, independently of gonadal hormonal levels, involving both trabecular and cortical bone. Of course, sex-specific age-related variation in bone mass is expected since bone loss accelerates during perimenopausal and postmenopausal years, as estrogen withdrawal around and after menopause promotes bone remodeling [86, 87]. This acceleration in bone loss around menopause is a leading determinant of the sex differences in the age-related patterns of bone loss [88].

Age estimation models based on BMD measured at the proximal femur are more accurate than those that rely in the metacarpal cortical index, individually or in conjugation. In sharp contrast with the proximal femur, the second metacarpal diaphysis is primarily composed by cortical bone, which is subjected to a slower remodeling due to its lower surface-area-to-volume ratio [86]. Interestingly, the best model (a GRNN model) to predict age at death in females employs both a predominantly cortical (femoral neck) and a mostly trabecular (Ward's area) ROI. In males, the best model is based upon Ward's area only (a GRNN model). Diagenesis (namely macrostructural, microstructural, or chemical variations of the bone) can influence the densitometric analyses. Hence, a previous evaluation of the possible effect of taphonomic factors on the densitometry readings is warranted. A mounting body of evidence suggests that, even in bones showing different degrees of diagenetic change, bone mineral content is not significantly modified [89, 90]. Direct and indirect evidence (macroscopical examination, lack of bone erosion caused by soil as shown on conventional radiographs, microradiography, and an epidemiologically expected pattern of bone loss) indicate that the studied sample presents a good state of preservation [1, 68, 91].

It is important to note that DXA is a more precise technique, while the sensitivity of conventional radiogrammetry regarding bone loss is restricted, as it can only detect a bone mass reduction of more than 30–50% [92]. It was noted in a French study that the cortical index shows a significant,

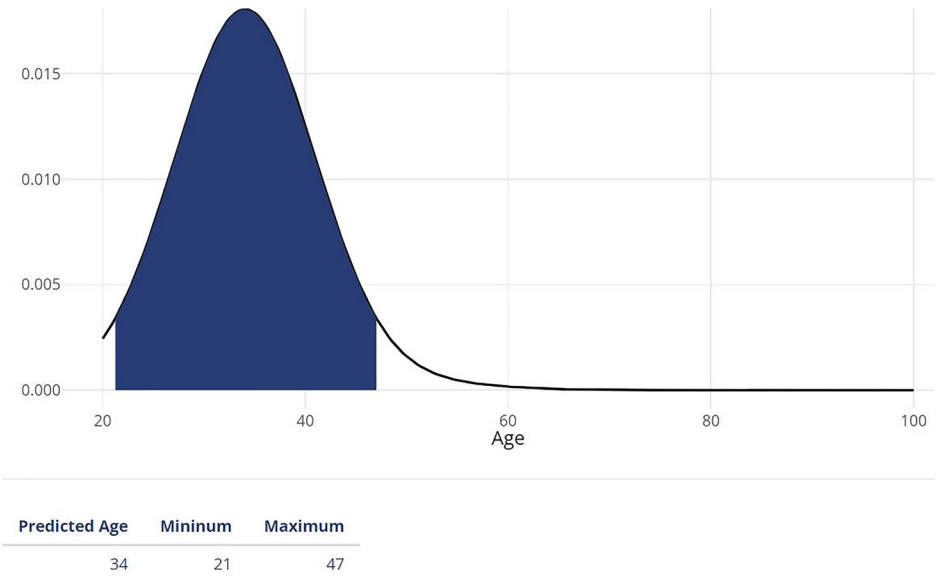

Fig. 4 DXAGE 2.0 is freely available at http://osteomics.com/DXAGE2/. DXAGE 2.0 displays the most probable point estimate for age at death, as well as a credible interval for the estimation

but poor, association with age in non-adults — in contrast, measurements of the epiphyseal-metaphyseal ratio (REM) presented a good correlation with age [65]. Notwithstanding, we have decided to maintain the models based on MCI, prioritizing applicability instead of accuracy, since, in certain circumstances, the second metacarpal may be the only bone available to estimate age at death.

Overall, GRNN models perform better than least squares regression models. By comparing similar models (i.e., models that feature the same variables), it is obvious that GRNN models present better goodness-of-fit statistics. For example, the mean absolute error in GRNN models ranges from 8.70 years (BMD Ward + MCI) to 12.58 years (MCI) in women, while in linear regression models, it varies from 9.39 years (BMD Ward + MCI) to 13.18 years (MCI). The difference is not impressive, but while least squares regression is a powerful and interpretable methodology, it shows some caveats — namely a detrimental effect by outliers and bias [93]. In fact, a well-recognized problem in adult age estimation — particularly when the dependent variable in linear regression is the age at death — is expressed by the "attraction of the middle," i.e., the systematic trend towards age overestimation in younger adults and age underestimation in older persons [34, 72, 94]. This trend has been recognized in different validation studies [95], including in an earlier method based in bone mineral density values [55]. The "age mimicry," specifically whereby age can be underestimated [94], can be magnified if the demographic composition of the reference sample does not include a large number of older individuals — and that is possibly the case for the males' sample in this study, particularly in the older age class (80 + years) that features only seven individuals. Different statistical approaches (e.g., Bayesian statistics, transition analysis or probabilistic models) have been employed to counteract estimation bias, e.g., [36, 37, 96–102].

Artificial neural networks are adaptative models that emulate the architecture of the brain [103, 104] and have been used to solve a plethora of generic tasks, being appropriate for modeling multifaceted and nonlinear phenomena [105]. ANN have been occasionally exploited in bioarcheology and forensic anthropology, but have shown their usefulness in applied purposes, such as sex estimation [106–109] and age prediction [35, 37, 98]. General regression neural networks are based on the general regression theory but operate as a black-box (however see Navega and Cunha, 2020), producing highly nonlinear functions with no interpretability constrains [111]. With the GRNN implementation, age at death is not simply estimated as a point value, but rather as a likely age interval.

A significant improvement of DXAGE 2.0 stems from the type of bones used to generate models for age estimation. The femur is among the strongest skeletal elements and one of the most abundant and well-preserved bones in archeological assemblages or forensic settings. The second metacarpal is less well represented in archeological contexts but tends to be well preserved and complete when present [112, 113]. This is particularly relevant since it is not always possible to use classic aging methods due to taphonomic factors [76, 114]. The pubic symphysis, for example, is extremely fragile and often does not resist to post-depositional processes [19]. Also, in the case of comingled and/or scattered remains, or mass disasters, individuals are usually represented by a subset of bones, or fragments of bone, severely limiting age at death assessment [115]. The study of commingled remains demands a larger degree of flexibility in the assessment of demographic features, such as age at death [116].

DXAGE 2.0 enables age estimation in incomplete or fragmentary skeletal remains — providing an additional tool to reconstruct the biological profile in different mortuary contexts, such as ossuaries, secondary burials, or mass graves. For example, crania and long bones compose the bulk of skeletal remains in ossuaries from protohistoric North America, characterized by multiple ritual steps during the mortuary treatment of the dead, or collective burials from the Late Neolithic in the Iberian Peninsula [117, 118]. Furthermore, techniques based in medical imaging modalities, including DXA, are non-invasive and suitable for age assessment in fleshed or partially fleshed cadaveric remains [56–58, 100, 119–124]. These are frequently recovered in forensic contexts and often skeletal preparation is not feasible, practical, or culturally acceptable. A DXA analysis of the proximal femur can also be used to estimate sex in skeletal remains [125–127]. Hence, an isolated femur has the potential to convey essential data about the major parameters of a biological profile, viz. age at death, sex, and stature.

Final remarks

Age at death estimation techniques have increasingly relied on more objective evaluations of the aging process combined with unconventional statistical approaches. Nevertheless, age estimation in adult skeletons is still fraught with difficulties, with individual and population factors influencing remodeling and degeneration of the skeleton and biological age. Accordingly, it is necessary to use different indicators to provide a more detailed and nuanced view of skeletal aging. DXAGE 2.0 yields comparable age estimates to those obtained by conventional methods, employing alternative skeletal regions, an objective analytic procedure, and providing an easy online platform for age prediction in adult skeletal remains. The proposed models show some limitations, particularly the fact that only individuals of south European ancestry were included in the training sample. Likewise, the relatively smaller sample of older males features a potential

methodological shortcoming. The addition of densitometric and radiogrammetric data from other populations, as well as from older individuals, to the current database of DXAGE 2.0 is thus desirable in future refinements.

Funding Portuguese Foundation for Science and Technology (FCT) (SFRH/BD/122306/2016).

Declarations

Ethical approval Not applicable.

Competing interests The authors declare no competing interests.

Research involving human participants and/or animals Not applicable.

Informed consent Not applicable.

References

1. Navega D, Coelho JdO, Cunha E, Curate F (2018) DXAGE: a new method for age at death estimation based on femoral bone mineral density and artificial neural networks. J Forensic Sci 63:497–503. https://doi.org/10.1111/1556-4029.13582
2. Ubelaker DH, Khosrowshahi H (2019) Estimation of age in forensic anthropology: historical perspective and recent methodological advances. Forensic Sci Res 4:1–9
3. Boldsen JL, Milner GR, Ousley SD (2021) Paleodemography: from archaeology and skeletal age estimation to life in the past. Am J Biol Anthropol. https://doi.org/10.1002/ajpa.24462
4. Stoyanova D, Algee-Hewitt BFB, Slice DE (2015) An enhanced computational method for age-at-death estimation based on the pubic symphysis using 3D laser scans and thin plate splines. Am J Phys Anthropol 158:431–440. https://doi.org/10.1002/ajpa.22797
5. Todd TW (1921) Age changes in the pubic bone. Am J Phys Anthropol 4:1–70. https://doi.org/10.1002/ajpa.1330040102
6. Brooks S, Suchey JM (1990) Skeletal age determination based on the os pubis: a comparison of the Acsádi-Nemeskéri and Suchey-Brooks methods. Hum Evol 5:227–238. https://doi.org/10.1007/BF02437238
7. Kim J, Algee-Hewitt BFB, Stoyanova DK et al (2019) Testing reliability of the computational age-at-death estimation methods between five observers using three-dimensional image data of the pubic symphysis. J Forensic Sci 64:507–518. https://doi.org/10.1111/1556-4029.13842
8. Castillo A, Galtés I, Crespo S, Jordana X (2021) Technical note: preliminary insight into a new method for age-at-death estimation from the pubic symphysis. Int J Legal Med 135:929–937. https://doi.org/10.1007/s00414-020-02434-6
9. Buckberry JL, Chamberlain AT (2002) Age estimation from the auricular surface of the ilium: a revised method. Am J Phys Anthropol 119:231–239. https://doi.org/10.1002/ajpa.10130
10. Lovejoy CO, Meindl RS, Pryzbeck TR, Mensforth RP (1985) Chronological metamorphosis of the auricular surface of the ilium : a new method for the determination of adult skeletal age at death 28:15–28
11. San Millán M, Rissech C, Turbón D (2013) A test of Suchey-Brooks (pubic symphysis) and Buckberry-Chamberlain (auricular surface) methods on an identified Spanish sample: paleodemographic implications. J Archaeol Sci 40:1743–1751. https://doi.org/10.1016/j.jas.2012.11.021
12. Nagaoka T, Hirata K (2008) Demographic structure of skeletal populations in historic Japan: a new estimation of adult age-at-death distributions based on the auricular surface of the ilium. J Archaeol Sci 35:1370–1377. https://doi.org/10.1016/j.jas.2007.10.002
13. Meindl RS, Lovejoy CO (1985) Ectocranial suture closure: a revised method for the determination of skeletal age at death based on the lateral-anterior sutures. Am J Phys Anthropol 68:57–66. https://doi.org/10.1002/ajpa.1330680106
14. Nawrocki SP (1998) Regression formulae for estimating age at death from cranial suture closure: a test of Meindl and Lovejoy's method. In: Reichs K (ed) Forensic osteology: advances in the identification of human remains. Charles C Thomas, Springfield, pp 276–292
15. İşcan MY, Loth SR, Wright RK (1984) Metamorphosis at the sternal rib end: a new method to estimate age at death in white males. Am J Phys Anthropol 65:147–156. https://doi.org/10.1002/ajpa.1330650206
16. İşcan MY, Loth SR, Wright RK (1985) Age estimation from the rib by phase analysis: white females. J Forensic Sci 30:11018J. https://doi.org/10.1520/jfs11018j
17. DiGangi EA, Bethard JD, Kimmerle EH, Konigsberg LW (2009) A new method for estimating age-at-death from the first rib. Am J Phys Anthropol 138:164–176. https://doi.org/10.1002/ajpa.20916
18. Mahlke NS, Renhart S, Talaa D et al (2021) Molecular clocks in ancient proteins: do they reflect the age at death even after millennia? Int J Legal Med 135:1225–1233. https://doi.org/10.1007/s00414-021-02522-1
19. Rissech C, Estabrook GF, Cunha E, Malgosa A (2006) Using the acetabulum to estimate age at death of adult males. J Forensic Sci 51:213–229. https://doi.org/10.1111/j.1556-4029.2006.00060.x
20. San-Millán M, Rissech C, Turbón D (2017) New approach to age estimation of male and female adult skeletons based on the morphological characteristics of the acetabulum. Int J Legal Med 131:501–525. https://doi.org/10.1007/s00414-016-1406-4
21. Griffin RC, Chamberlain AT, Hotz G et al (2009) Age estimation of archaeological remains using amino acid racemization in dental enamel: a comparison of morphological, biochemical, and known ages-at-death. Am J Phys Anthropol 140:244–252. https://doi.org/10.1002/ajpa.21058
22. Ritz S, Schütz H-W (1993) Aspartic acid racemization in intervertebral discs as an aid to postmortem estimation of age at death. J Forensic Sci 38:13449J. https://doi.org/10.1520/jfs13449j
23. Lamendin H, Baccino E, Humbert JF et al (1992) A simple technique for age estimation in adult corpses: the two criteria dental method. J Forensic Sci 37:13327J. https://doi.org/10.1520/jfs13327j
24. Prince DA, Kimmerle EH, Konigsberg LW (2008) A Bayesian approach to estimate skeletal age-at-death utilizing dental wear. J Forensic Sci 53:588–593. https://doi.org/10.1111/j.1556-4029.2008.00714.x
25. Brothwell D (1981) Digging up bones, 3rd edn. Oxford University Press, Oxford
26. De Luca S, Alemán I, Bertoldi F et al (2010) Age estimation by tooth/pulp ratio in canines by peri-apical X-rays: reliability in age determination of Spanish and Italian medieval skeletal remains. J Archaeol Sci 37:3048–3058. https://doi.org/10.1016/j.jas.2010.06.034
27. Thomas CDL, Stein MS, Feik SA et al (2000) Determination of age at death using combined morphology and histology of the femur. J Anat 196:463–471. https://doi.org/10.1046/j.1469-7580.2000.19630463.x

28. Botha D, Steyn M, Lynnerup N (2019) Histological age-at-death estimation in white South Africans using stereology. Int J Legal Med 133:1957–1965. https://doi.org/10.1007/s00414-019-02152-8
29. Mays S (2015) The effect of factors other than age upon skeletal age indicators in the adult. Ann Hum Biol 42:330–339. https://doi.org/10.3109/03014460.2015.1044470
30. Buckberry J (2015) The (mis)use of adult age estimates in osteology. Ann Hum Biol 42:321–329. https://doi.org/10.3109/03014460.2015.1046926
31. Wescott DJ, Drew JL (2015) Effect of obesity on the reliability of age-at-death indicators of the pelvis. Am J Phys Anthropol 156:595–605. https://doi.org/10.1002/ajpa.22674
32. Zapico SC, Ubelaker DH (2013) Applications of physiological bases of ageing to forensic sciences. Estimation of age-at-death Ageing Res Rev 12:605–617. https://doi.org/10.1016/j.arr.2013.02.002
33. Garvin HM, Passalacqua NV (2012) Current practices by forensic anthropologists in adult skeletal age estimation. J Forensic Sci 57:427–433
34. Bocquet-Appel JP, Masset C (1982) Farewell to paleodemography. J Hum Evol 11:321–333. https://doi.org/10.1016/S0047-2484(82)80023-7
35. Corsini MM, Schmitt A, Bruzek J (2005) Aging process variability on the human skeleton: artificial network as an appropriate tool for age at death assessment. Forensic Sci Int 148:163–167. https://doi.org/10.1016/j.forsciint.2004.05.008
36. Boldsen JL, Milner GR, Konigsberg LW, Wood J (2002) Transition analysis: a new method for estimating age from skeletons. In: Hoppa R, Vaupel J (eds) Paleodemography: age distributions from skeletal samples. Cambridge University Press, Cambridge, pp 73–106
37. Kotěrová A, Navega D, Štepanovský M et al (2018) Age estimation of adult human remains from hip bones using advanced methods. Forensic Sci Int 287:163–175. https://doi.org/10.1016/j.forsciint.2018.03.047
38. J d'Oliveira Coelho F Curate D Navega 2020 Osteomics: decision support systems for forensic anthropologists Stat Probab Forensic Anthropol 259–273https://doi.org/10.1016/b978-0-12-815764-0.00005-8
39. El Maghraoui A, Guerboub AA, Achemlal L et al (2006) Bone mineral density of the spine and femur in healthy Moroccan women. J Clin Densitom 9:454–460. https://doi.org/10.1016/j.jocd.2006.07.001
40. LookerLG AB, Hughes J et al (2012) Lumbar spine and proximal femur bone mineral density, bone mineral content, and bone area: United States, 2005–2008. Vital Heal Stat 11:1–132
41. Sheu Y, Cauley JA, Wheeler VW et al (2011) Age-related decline in bone density among ethnically diverse older men. Osteoporos Int 22:599–605. https://doi.org/10.1007/s00198-010-1330-2
42. Lee KS, Bae SH, Lee SHw et al (2014) New reference data on bone mineral density and the prevalence of osteoporosis in Korean adults aged 50 years or older: the Korea National Health and Nutrition Examination Survey 2008–2010. J Korean Med Sci 29:1514–1522. https://doi.org/10.3346/jkms.2014.29.11.1514
43. Aggarwal A, Pal R, Bhadada SK et al (2021) Bone mineral density in healthy adult Indian population: the Chandigarh Urban Bone Epidemiological Study (CUBES). Arch Osteoporos 16:17
44. Naik AA, Xie C, Zuscik MJ et al (2009) Reduced COX-2 expression in aged mice is associated with impaired fracture healing. J Bone Miner Res 24:251–264. https://doi.org/10.1359/jbmr.081002
45. Riggs BL (2003) Role of the vitamin D-endocrine system in the pathophysiology of postmenopausal osteoporosis. J Cell Biochem 88:209–215. https://doi.org/10.1002/jcb.10345
46. Vashishth D, Tanner KE, Bonfield W (2003) Experimental validation of a microcracking-based toughening mechanism for cortical bone. J Biomech 36:121–124. https://doi.org/10.1016/S0021-9290(02)00319-6
47. Schranz D (1959) Age determination from the internal structure of the humerus. Am J Phys Anthropol 17:273–277. https://doi.org/10.1002/ajpa.1330170403
48. Walker RA, Lovejoy CO (1985) Radiographic changes in the clavicle and proximal femur and their use in the determination of skeletal age at death. Am J Phys Anthropol 68:67–78. https://doi.org/10.1002/ajpa.1330680107
49. Bergot C, Bocquet J-P (1976) Etude systématique, en fonction de l'âge, de l'os spongieux et de l'os cortical de l'humérus et du fémur. Bull Mem Soc Anthropol Paris 3:215–242. https://doi.org/10.3406/bmsap.1976.1852
50. Kimura K (1992) Estimation of age at death from second metacarpals. Z Morphol Anthropol 79:169–181. https://doi.org/10.1127/zma/79/1992/169
51. Macchiarelli R, Bondioli L (1994) Linear densitometry and digital image processing of proximal femur radiographs: implications for archaeological and forensic anthropology. Am J Phys Anthropol 93:109–122. https://doi.org/10.1002/ajpa.1330930108
52. Szilvássy J, Kritscher H (1990) Estimation of chronological age in man based on the spongy structure of long bones. Anthropol Anzeiger 48:289–298. https://doi.org/10.1127/anthranz/48/1990/289
53. Fisher E, Austin D, Werner HM et al (2016) Hyoid bone fusion and bone density across the lifespan: prediction of age and sex. Forensic Sci Med Pathol 12:146–157. https://doi.org/10.1007/s12024-016-9769-x
54. Todd TW (1930) Age changes in the pubic bone. VIII. Roentgenographic differentiation Am J Phys Anthropol 14:255–271. https://doi.org/10.1002/ajpa.1330140205
55. Curate F, Albuquerque A, Cunha EM (2013) Age at death estimation using bone densitometry: testing the Fernández Castillo and López Ruiz method in two documented skeletal samples from Portugal. Forensic Sci Int 226:296.e1-296.e6. https://doi.org/10.1016/j.forsciint.2012.12.002
56. Fernández Castillo R, López Ruiz MC (2011) Assessment of age and sex by means of DXA bone densitometry: application in forensic anthropology. Forensic Sci Int 209:53–58. https://doi.org/10.1016/j.forsciint.2010.12.008
57. Paschall A, Ross AH (2018) Biological sex variation in bone mineral density in the cranium and femur. Sci Justice 58:287–291. https://doi.org/10.1016/j.scijus.2018.01.002
58. Botha D, Lynnerup N, Steyn M (2019) Age estimation using bone mineral density in South Africans. Forensic Sci Int 297:307–314. https://doi.org/10.1016/j.forsciint.2019.02.020
59. Curate F, Perinha A, Silva AM et al (2019) Metacarpal cortical bone loss and osteoporotic fractures in the Coimbra Identified Skeletal Collection. Int J Osteoarchaeol 29:73–81. https://doi.org/10.1002/oa.2717
60. Mays S (1996) Age-dependent cortical bone loss in a medieval population. Int J Osteoarchaeol 6:144–154. https://doi.org/10.1002/(SICI)1099-1212(199603)6:2%3c144::AID-OA261%3e3.0.CO;2-G
61. Mays S (2000) Age-dependent cortical bone loss in women from 18th and early 19th century London. Am J Phys Anthropol 112:349–361. https://doi.org/10.1002/1096-8644(200007)112:3%3c349::AID-AJPA6%3e3.0.CO;2-0
62. Shepherd JA, Meta M, Landau J et al (2005) Metacarpal index and bone mineral density in healthy African-American women. Osteoporos Int 16:1621–1626. https://doi.org/10.1007/s00198-005-1885-5

63. Virtama P, Helelä T (1969) Radiographic measurements of cortical bone: variations in a normal population between 1 and 90 years of age. Acta radiol 1–268
64. Ives R, Brickley M (2005) Metacarpal radiogrammetry: a useful indicator of bone loss throughout the skeleton? J Archaeol Sci 32:1552–1559. https://doi.org/10.1016/j.jas.2005.04.008
65. Faruch Bilfeld M, Dedouit F, Soumah M et al (2008) Apport de la radiographie du second métacarpien pour la détermination de l'âge osseux. J Radiol 89:1930–1934. https://doi.org/10.1016/S0221-0363(08)74789-9
66. Cunha E, Wasterlain S (2007) The Coimbra identified osteological collections. In: Grupe G, Peters J (eds) Skeletal series in their socioeconomic context. M. Leidorf, Rahden/Westphalia, pp 23–33
67. Bonnick SL, Lewis LA (2013) Bone densitometry for technologists, 3rd edn. Human Press, Tottowa
68. Curate F, Albuquerque A, Correia J et al (2013) A glimpse from the past: osteoporosis and osteoporotic fractures in a portuguese identified skeletal sample. Acta Reumatol Port 38:20–27
69. Ives R, Brickley MB (2004) A procedural guide to metacarpal radiogrammetry in archaeology. Int J Osteoarchaeol 14:7–17. https://doi.org/10.1002/oa.709
70. Larose CD, Larose DT (2019) Data science using Python and R. John Wiley & Sons Inc, Hoboken, NJ
71. Specht DF (1991) A general regression neural network. IEEE Trans Neural Networks 2:568–576. https://doi.org/10.1109/72.97934
72. Aykroyd RG, Lucy D, Pollard AM, Solheim T (1997) Technical note: regression analysis in adult age estimation 265:259–265
73. Besalú E (2013) The connection between inverse and classical calibration. Talanta 116:45–49. https://doi.org/10.1016/j.talanta.2013.04.054
74. Jobran Al-Mahasneh A, Anavatti S, Garratt and Mahardhika Pratama M (2018) Applications of general regression neural networks in dynamic systems. In: Asadpour V (ed) Digital systems. IntechOpen, Rijeka
75. Konigsberg LW, Herrmann NP, Wescott DJ, Kimmerle EH (2008) Estimation and evidence in forensic anthropology: age-at-death. J Forensic Sci 53:541–557. https://doi.org/10.1111/j.1556-4029.2008.00710.x
76. Rougé-Maillart C, Vielle B, Jousset N et al (2009) Development of a method to estimate skeletal age at death in adults using the acetabulum and the auricular surface on a Portuguese population. Forensic Sci Int 188:91–95. https://doi.org/10.1016/j.forsciint.2009.03.019
77. Makker A, Mishra G, Singh BP et al (2008) Normative bone mineral density data at multiple skeletal sites in Indian subjects. Arch Osteoporos 3:25–37. https://doi.org/10.1007/s11657-008-0019-z
78. Tokida R, Uehara M, Nakano M et al (2021) Reference values for bone metabolism in a Japanese cohort survey randomly sampled from a basic elderly resident registry. Sci Rep 11:7822. https://doi.org/10.1038/s41598-021-87393-7
79. Lees B, Stevenson JC, Molleson T, Arnett TR (1993) Differences in proximal femur bone density over two centuries. Lancet 341:673–676. https://doi.org/10.1016/0140-6736(93)90433-H
80. Chen KK, Wee SL, Pang BWJ, et al (2020) Bone mineral density reference values in Singaporean adults and comparisons for osteoporosis establishment - the Yishun Study. BMC Musculoskelet. Disord. 21
81. Dequeker J, Leuven AH, Leuven KU (1975) Occasional survey bone and ageing. Ann Rheum Dis 34:100–115
82. Whitmarsh T, Otake Y, Uemura K et al (2019) A cross-sectional study on the age-related cortical and trabecular bone changes at the femoral head in elderly female hip fracture patients. Sci Rep 9:1–8. https://doi.org/10.1038/s41598-018-36299-y
83. Cheuk KY, Wang XF, Wang J et al (2018) Sexual dimorphism in cortical and trabecular bone microstructure appears during puberty in Chinese children. J Bone Miner Res 33:1948–1955. https://doi.org/10.1002/jbmr.3551
84. Seeman E (2008) Structural basis of growth-related gain and age-related loss of bone strength. Rheumatology 47:2–8. https://doi.org/10.1093/rheumatology/ken177
85. Iuliano-Burns S, Hopper J, Seeman E (2009) The age of puberty determines sexual dimorphism in bone structure: a male/female co-twin control study. J Clin Endocrinol Metab 94:1638–1643. https://doi.org/10.1210/jc.2008-1522
86. Isales C, Seeman E (2019) Menopause and age-related bone loss. In: Bilezikian J (ed) Primer on the metabolic bone diseases and disorders of mineral metabolism, 9th edn. John Wiley & Sons, Hoboken, pp 155–161
87. Khosla S (2013) Pathogenesis of age-related bone loss in humans. J Gerontol - Ser A Biol Sci Med Sci 68:1226–1235. https://doi.org/10.1093/gerona/gls163
88. Berger C, Langsetmo L, Joseph L et al (2009) Association between change in BMD and fragility fracturein women and men. J Bone Miner Res 24:361–370. https://doi.org/10.1359/jbmr.081004
89. Spinek AE, Lorkiewicz W, Mietlińska J et al (2016) Evaluation of chronological changes in bone fractures and age-related bone loss: a test case from Poland. J Archaeol Sci 72:117–127. https://doi.org/10.1016/j.jas.2016.06.007
90. Turner-Walker G, Syversen U (2002) Quantifying histological changes in archaeological bones using BSE-SEM image analysis. Archaeometry 44:461–468. https://doi.org/10.1111/1475-4754.t01-1-00078
91. Bergot C, Wu Y, Jolivet E et al (2009) The degree and distribution of cortical bone mineralization in the human femoral shaft change with age and sex in a microradiographic study. Bone 45:435–442. https://doi.org/10.1016/j.bone.2009.05.025
92. Jensen T, Klarlund M, Hansen M et al (2004) Bone loss in unclassified polyarthritis and early rheumatoid arthritis is better detected by digital x ray radiogrammetry than dual x ray absorptiometry: relationship with disease activity and radiographic outcome. Ann Rheum Dis 63:15–22. https://doi.org/10.1136/ard.2003.013888
93. Larose D, Larose C (2015) Data mining and predictive analytics. John Wiley & Sons, Hoboken, NJ
94. Masset C (1989) Age estimation based on cranial sutures. In: Iscan MY (ed) Age markers in the human skeleton. CC Thomas, Springfield, pp 71–103
95. M Vossoughi N Movahhedian A Ghafoori 2021 The impact of age mimicry bias on the accuracy of methods for age estimation based on Kvaal's pulp/tooth ratios: a bootstrap study Int J Legal Med https://doi.org/10.1007/s00414-021-02651-7
96. Lucy D, Aykroyd RG, Pollard AM (2002) Nonparametric calibration for age estimation. J R Stat Soc Ser C Appl Stat 51:183–196. https://doi.org/10.1111/1467-9876.00262
97. Dudzik B, Langley NR (2015) Estimating age from the pubic symphysis: a new component-based system. Forensic Sci Int 257:98–105. https://doi.org/10.1016/j.forsciint.2015.07.047
98. Buk Z, Kordik P, Bruzek J et al (2012) The age at death assessment in a multi-ethnic sample of pelvic bones using nature-inspired data mining methods. Forensic Sci Int 220:294.e1-294.e9. https://doi.org/10.1016/j.forsciint.2012.02.019
99. Milner GR, Boldsen JL (2012) Transition analysis: a validation study with known-age modern American skeletons. Am J Phys Anthropol 148:98–110. https://doi.org/10.1002/ajpa.22047
100. Aramaki T, Ikeda T, Usui A, Funayama M (2017) Age estimation by ossification of thyroid cartilage of Japanese males using Bayesian analysis of postmortem CT images. Leg Med 25:29–35. https://doi.org/10.1016/j.legalmed.2016.12.001

101. Kim J, Algee-Hewitt BFB (2022) Age-at-death patterns and transition analysis trends for three Asian populations: implications for [paleo]demography. Am J Biol Anthropol 177:207–222. https://doi.org/10.1002/ajpa.24419
102. Jooste N, Pretorius S, Steyn M (2022) Performance of three mathematical models for estimating age-at-death from multiple indicators of the adult skeleton. Int J Legal Med 136:739–751. https://doi.org/10.1007/s00414-021-02727-4
103. Abdi H, Valentin D, Edelman B (1999) Neural networks. Sage Publications, Thousand Oaks
104. Deravignioni L, Macchi Jánica G (2006) Artificial neural networks in archaeology. Archeol e Calc 17:121–136. https://doi.org/10.1142/9789812778055_0008
105. Yang ZR, Yang Z (2014) Artificial neural networks. In: Brahme A (ed) Comprehensive biomedical physics. Elsevier B.V., Radarweg, pp 1–17
106. Cavalli F, Lusnig L, Trentin E (2017) Use of pattern recognition and neural networks for non-metric sex diagnosis from lateral shape of calvarium: an innovative model for computer-aided diagnosis in forensic and physical anthropology. Int J Legal Med 131:823–833. https://doi.org/10.1007/s00414-016-1439-8
107. du Jardin P, Ponsaille J, Alunni-Perret V, Quatrehomme G (2009) A comparison between neural network and other metric methods to determine sex from the upper femur in a modern French population. Forensic Sci Int 192:127.e1-127.e6. https://doi.org/10.1016/j.forsciint.2009.07.014
108. Mahfouz M, Badawi A, Merkl B et al (2007) Patella sex determination by 3D statistical shape models and nonlinear classifiers. Forensic Sci Int 173:161–170. https://doi.org/10.1016/j.forsciint.2007.02.024
109. Navega D, Vicente R, Vieira DN et al (2015) Sex estimation from the tarsal bones in a Portuguese sample : a machine learning approach. Int J Legal Med 129:651–659. https://doi.org/10.1007/s00414-014-1070-5
110. Navega D, Cunha E (2020) Extreme learning machine neural networks for adult skeletal age-at-death estimation. In: Obertová Z, Stewart A, Cattaneo C (eds) Statistics and probability in forensic anthropology. Academic Press, London, pp 209–225
111. Li O, Liu H, Chen C, Rudin C (2018) Deep learning for case-based reasoning through prototypes: a neural network that explains its predictions. In: 32nd AAAI Conference on Artificial Intelligence, AAAI 2018. pp 3530–3537
112. Bello S, Andrews P (2006) The intrinsic pattern of preservation of human skeletons and its influence on the interpretation of funerary behaviours. Soc Archaeol Funer Remain 1–13
113. Mays S (1992) Taphonomic factors in a human skeletal assemblage. Circaea 9:54–58
114. Cappella A, Cummaudo M, Arrigoni E et al (2017) The issue of age estimation in a modern skeletal population: are even the more modern current aging methods satisfactory for the elderly? J Forensic Sci 62:12–17. https://doi.org/10.1111/1556-4029.13220
115. Baccino E, Schmitt A (2006) Determination of adult age at death in the forensic context. In: Schmitt A, Cunha EM, Pinheiro J (eds) Forensic anthropology and medicine: complementary sciences from recovery to cause of death. Humana Press, Tottowa, pp 259–280
116. Baustian KM, Osterholtz AJ, Cook DC (2014) Taking analyses of commingled remains into the future: challenges and prospects. In: Commingled and disarticulated human remains: working toward improved theory, method, and data. pp 265–274
117. Silva AM (2003) Portuguese populations of late Neolithic and Chalcolithic periods exhumed from collective burials: an overview. Anthropol 41:55–64
118. Ubelaker DH (1974) Reconstruction of demographic profiles from ossuary skeletal samples
119. Carneiro C, Curate F, Cunha E (2016) A method for estimating gestational age of fetal remains based on long bone lengths. Int J Legal Med 130:1333–1341. https://doi.org/10.1007/s00414-016-1393-5
120. Sinanoglu A, Kocasarac HD, Noujeim M (2016) Age estimation by an analysis of spheno-occipital synchondrosis using cone-beam computed tomography. Leg Med 18:13–19. https://doi.org/10.1016/j.legalmed.2015.11.004
121. Dubourg O, Faruch-Bilfeld M, Telmon N et al (2020) Technical note: age estimation by using pubic bone densitometry according to a twofold mode of CT measurement. Int J Legal Med 134:2275–2281. https://doi.org/10.1007/s00414-020-02349-2
122. Schanandore JV, Ford JM, Decker SJ (2018) Correlation between chronological age and computed tomography attenuation of trabecular bone from the os coxae. J Forensic Radiol Imaging 14:24–31. https://doi.org/10.1016/j.jofri.2018.08.006
123. Bascou A, Dubourg O, Telmon N et al (2021) Age estimation based on computed tomography exploration: a combined method. Int J Legal Med 135:2447–2455. https://doi.org/10.1007/s00414-021-02666-0
124. Fan F, Tu M, Li R et al (2020) Age estimation by multidetector computed tomography of cranial sutures in Chinese male adults. Am J Phys Anthropol 171:550–558. https://doi.org/10.1002/ajpa.23998
125. Curate F, Albuquerque A, Ferreira I, Cunha E (2017) Sex estimation with the total area of the proximal femur: a densitometric approach. Forensic Sci Int 275:110–116. https://doi.org/10.1016/j.forsciint.2017.02.035
126. Meeusen RA, Christensen AM, Joseph T, Hefner (2015) The use of femoral neck axis length to estimate sex and ancestry. J Forensic Sci 60:1300–1304. https://doi.org/10.1111/1556-4029.12820
127. Wheatley BP (2005) An evaluation of sex and body weight determination from the proximal femur using DXA technology and its potential for forensic anthropology 147:141–145. https://doi.org/10.1016/j.forsciint.2004.09.076